Biogeochemical Processes Controlling Microbial Reductive Precipitation of Radionuclides

PIs: James K. Fredrickson[1] and Scott C. Brooks[2]

Contributors: Sue L. Carroll[2], Scott Fendorf[4], Shelly D. Kelly[3], Kenneth M. Kemner[3], Alice Dohnalkova[1], Alex Beliaev[1], David W. Kennedy[1], Yuri A. Gorby[1], and John M. Zachara[1]

[1]Pacific Northwest National Laboratory, Richland, WA, [2]Oak Ridge National Laboratory, Oak Ridge, TN

[3]Argonne National Laboratory, Argonne, IL, [4]Stanford University, Palo Alto, CA

Project Objectives

This project is focused on elucidating the principal biogeochemical reactions that govern the concentrations, chemical speciation, and distribution of the redox sensitive contaminants uranium (U) and technetium (Tc) between the aqueous and solid phases. The research is designed to provide new insights into the under-explored areas of competing geochemical and microbiological oxidation-reduction reactions that govern the fate and transport of redox sensitive contaminants and to generate fundamental scientific understanding of the identity and stoichiometry of competing microbial reduction and geochemical oxidation reactions. These goals and objectives are met through a series of hypothesis-driven tasks that focus on (1) the use of well-characterized microorganisms and synthetic and natural mineral oxidants, (2) advanced spectroscopic and microscopic techniques to monitor redox transformations of U and Tc, and (3) the use of flow-through experiments to more closely approximate groundwater environments. The results are providing an improved understanding and predictive capability of the mechanisms that govern the redox dynamics of radionuclides in subsurface environments. For purposes of this poster, the results are divided into three sections: I. influence of Ca on U(VI) bioreduction; II. localization of biogenic UO_2 and TcO_2; and III. reactivity of Mn(III/IV) oxides.

Background

Defense related activities have resulted in vast areas of U and Tc contaminated soils and groundwater across the DOE complex. Oxidized uranium (VI) and Tc(VII) have relatively high solubilities but are readily reduced by a variety of metal reducing bacteria (MRB) under anoxic conditions to U(IV) and Tc(IV) with subsequent precipitation of uraninite U(IV)O_2 or hydrous TcO_2. The low solubility of these hydrous oxides makes bioremediation an attractive option for removing U and Tc from contaminated groundwater.

I. Influence of Ca on U(VI) Bioreduction

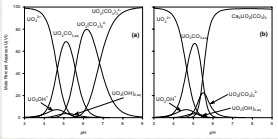

Figure 1: Predicted U(VI) aqueous species distribution neglecting (a) and including (b) the Ca-UO_2-CO_3 complexes. Consideration of the ternary species results in a major shift in aqueous species distribution starting at pH values > 5. U_{TOT} = 10 μM; TIC = 10 mM; Ca_{TOT} = 5 mM, concentration values which are commonly encountered at the NABIR Field Research Center and UMTRA sites.

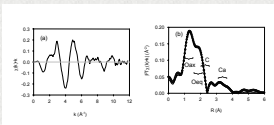

Figure 2: (a) XAFS $\chi(k) \cdot k$ data for Ca-containing base solution. (b) Magnitude of the Fourier transform of the data shown in 2a (open circles) and best-fit model (thick line). Data processed with Δk = 3.3-9.3 Å^{-1}, ΔR = 0.9-4.0 Å, and a Hanning window with a full sill width of 1.0 Å^{-1}.

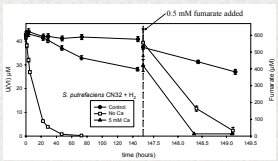

Figure 3: Reduction of U(VI) by *S. putrefaciens* CN32 in the absence and presence of Ca followed by the addition of 0.5 mM fumarate as an electron acceptor. Fumarate was rapidly removed from treatments with lactate indicating cells in the presence and absence of Ca were equally active.

Key Findings:

- **Ca at environmentally relevant concentrations significantly decreased the rate & extent of bacterial (*Shewanella*, *Geobacter*, *Desulfovibrio*) U reduction but did not impact Tc or fumarate reduction.**
- **XAFS analyses indicated a structure consistent with a Ca-UO_2-CO_3 complex.**
- **Ca-UO_2-CO_3 is proposed to be a less energetically favorable e^- acceptor than other common U(VI) complexes.**
- **Ca concentrations at the ORNL FRC range from 1-300 mM and hence could impact U bioreduction at this site.**

Brooks, S. C., J. K. Fredrickson, S. L. Carroll, D. W. Kennedy, J. M. Zachara, A. E. Plymale, and S. Fendorf. 2003. Inhibition of bacterial U(VI) reduction by calcium. *Environ. Sci. Technol.* **37:**1850-1858.

II. Localization of Biogenic UO_2

Background

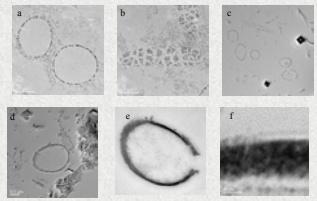

Figure 4: TEM images of unstained thin sections from *S. putrefaciens* CN32 cells incubated with H_2 and U(VI) in bicarbonate buffer in the absence of Mn oxides illustrating the accumulation of U(IV) extracellularly and in the periplasm (a) and after staining with uranyl acetate to more clearly reveal cell ultrastructure (b). CN32 incubated with H_2 and U(VI) in the presence of bixbyite (Mn_2O_3) (c) or birnessite (δ-MnO_2) (d) exhibited an absence of fine-grained extracellular UO_2 (c) and accumulation of UO2 almost exclusively in the periplasm (e, f) (Fredrickson et al. 2003). Results demonstrate that accumulation in the periplasm can protect UO_2 against oxidation by Mn(IV).

Current Research

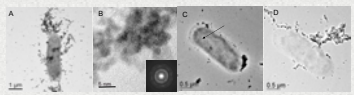

Figure 5: SEM micrographs of an unstained whole mount of MR-1 following incubation with 250 μM uranyl acetate and 10 cc of H_2 for 48 h (A) and high resolution TEM image of extracellular UO_2 nanoparticles (B); the inset SAED pattern is consistent with previous patterns of biogenic and synthetic UO_2. Upon close inspection of the cell surface, electron dense spots (U) are regularly distributed over the cell surface and are surrounded by ring-shaped structures (arrow in C, D).

An insertional mutant in *gspD*, a component of the type II protein secretion pathway (T2S), was generated in MR-1 and evaluated U reduction and localization. GspD is an integral membrane protein that belongs to the secretin superfamily and forms a stable ring-shaped complex of 12-14 subunits in the outer membrane of Gram-negative bacteria. The central channel of the GspD secretin is approximately 5-10 nm in diameter, large enough to allow the secretion of folded proteins across the outer membrane. A complete Type II secretion (T2S) pathway is present in the genome of *S. oneidensis* MR-1.

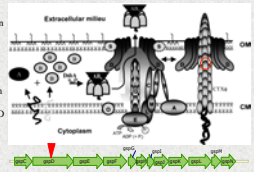

From Sandkvist, M. Mol. Microbiol. 2001. 40(2):271-283.

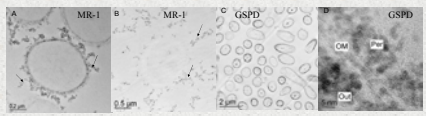

Figure 6: TEM micrographs of thin sections prepared from cell suspensions incubated with 250 μM uranyl acetate and 10 cc of H_2 and then fixed, dehydrated, embedded, and sectioned under an inert atmosphere. Sections are from MR-1 cells incubated for 8 (A) and 48 (B) h and GSPD incubated for 48 h (C) and high magnification images of the GSPD cell envelope (D). Note the accumulation of UO_2 external to the cell in MR-1 in association with fiber-like features and the lack of these features in GSPD with a heavy accumulation in the periplasm.

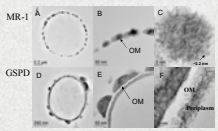

Figure 7: TEM micrographs of thin sections prepared from cell suspensions incubated with 250 μM NH_4TcO_4 and 10 cc of H_2 and then fixed, dehydrated, embedded, and sectioned under an inert atmosphere. Sections are from MR-1 (A, B, C) and GSPD (D, E, F) cells incubated for 5 d. Note the accumulation of TcO_2 outside the periplasm in MR-1 and in the periplasm in GSPD.

Key Findings:

- **Reduction of U(VI) by MR-1 results in extracellular accumulation of UO_2 nanoparticles (~ 5 nm), some in association with fiber-like structures (see Y.A. Gorby poster)**
- **A mutant in the T2S pathway (*gspD*) accumulated UO_2 in the periplasm and at the OM surface. [Note: T. DiChristina has shown that a *gspE* mutant in *S. putrefaciens* is deficient in Fe & Mn reduction]**
- **In MR-1, TcO_2 accumulated outside of the OM as ~2.2 nm particles in patches 20-30 nm in diameter. In GSPD, TcO_2 accumulated in the periplasm and as mushroom-shaped structures on the OM.**
- **The *gspD* mutant may be unable to export reduced nanoparticles form the periplasm, unable to secrete metal-reducing proteins to the cell surface, or both.**
- **These results have implications for the fate and long-term stability of bioreduced contaminants.**

Fredrickson, J. K., J. M. Zachara, D. W. Kennedy, C. Liu, M. C. Duff, D. B. Hunter, and A. Dohnalkova. 2002. Influence of Mn oxides on the reduction of Uranium(VI) by the metal-reducing bacterium *Shewanella putrefaciens*. *Geochim. Cosmochim. Acta* **66:**3247-3262.

III. Reactivity of Mn(III/IV) Oxides

Oxidation of Biogenic Uraninite ($(U^{IV}_{0.91}U^{VI}_{0.09})O_{2.09}$)) by Mn Oxides

Initial conditions: 250 μM U_{TOT}; 100 m^2/L Mn oxide; in 30 mM $NaHCO_3$ + 20% $CO_{2(g)}$; pH 7

Mineral	Ratio Mn : U(VI) Predicted	Ratio Mn : U(VI) Measured (± 1 std error)	Initial Rate (μM/h) (± 1 std error)	Pseudo 1st Order k (h^{-1}) (± 1 std error)
Hausmannite (Mn_3O_4)	**2.73**	--	**12 ± 2**	**0.024 ± 0.002**
Manganite (γ-MnOOH)	**1.82**	**1.93 ± 0.23**	**14 ± 1**	**0.025 ± 0.004**
Bixbyite (Mn_2O_3)	**1.75**	**1.78 ± 0.04**	**15 ± 2**	**0.019 ± 0.002**
HMO ($MnO_{2.nH_2O}$)	**0.94**	**0.86 ± 0.15**	**2.1 ± 0.9***	**0.025 ± 0.004***
Nsutite (γ-MnO_2)	**1.14**	**1.14 ± 0.07**	**5.3 ± 0.6**	**0.020 ± 0.004**

*Autocatalytic reaction – see Figure 9 below

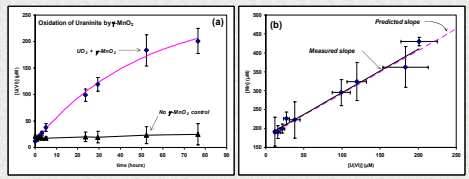

Figure 8: Oxidation of biogenic uraninite by γ-MnO_2. (a) the data are described well by a pseudo-first order production curve (pink line). The observed lack of production of U(VI) in no Mn oxide controls confirms the exclusion of oxygen from the experimental system (biogenic uraninite contained ~10% U(VI)). (b) Measured ratio of Mn to U(VI) produced agreed well with the ratio predicted based on the independently measured oxidation state of U and Mn in the original solids. (data points and error bars represent the mean ± 1 std error).

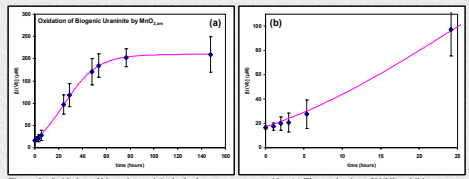

Figure 9. Oxidation of biogenic uraninite by hydrous manganese oxide. (a) The production of U(VI) exhibits characteristics of an autocatalytic reaction. The initial rate is slower than at intermediate times when a catalytic product has accumulated; the rate eventually slows down as reactant (UO_2) is consumed. (b) Close-up view of early time data. Data points and error bars are the mean ± 1s, line is fitted autocatalytic kinetic model.

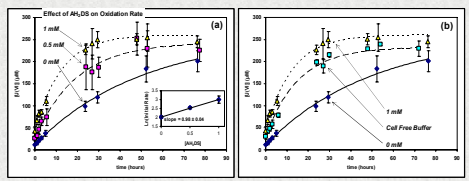

Figure 10: (a) The anaerobic pre-reduction of γ-MnO_2 with bioreduced AH_2DS significantly increases the rate of U(IV) oxidation. The initial rate of U(VI) production exhibits a first-order dependence on the concentration of AH_2DS (inset to panel (a)). The mechanism for the enhanced rate is presently unclear; pre-treatment with an equivalent amount of Mn(II) has no impact on the rate of oxidation (controls receiving anaerobic water show no U(VI) production confirming anaerobic conditions). (b) However, anaerobic pre-treatment with cell-free buffer used to harvest and re-suspend cultured cells that contains no AH_2DS results in a significant increase in the rate of U(VI) production.

Key Findings:

- **Mn(III/IV) oxides rapidly and completely oxidize biogenic uraninite.**
- **Mn(III) oxides sustain a faster initial rate of U(VI) production than Mn(IV) oxides when compared on an equal surface area basis.**
- **The production of U(VI) in the presence of amorphous MnO_2 exhibits autocatalytic behavior, in which the rate of U(IV) oxidation increases at intermediate times and slows as U(IV) is consumed.**
- **Pre-reduction of γ-MnO2 with bioreduced AH2DS or pretreatment with cell free resuspension buffer results in a significantly faster rate of U(IV) oxidation.**
- **These results potentially have significant implication with respect to the long-term immobilization of U as biogenic U(IV) precipitates in subsurface environments.**

Acknowledgments - This research was supported by the Natural and Accelerated Bioremediation Research Program (NABIR), Office of Biological and Environmental Research, U.S. Department of Energy (DOE). (We'll miss you Anna!)